Journal of Volcanology and Geothermal Research 386 (2019) 106672

Contents lists available at ScienceDirect

Journal of Volcanology and Geothermal Research

journal homepage: www.elsevier.com/locate/jvolgeores

Mantle earthquakes beneath Fogo volcano, Cape Verde: Evidence for subcrustal fracturing induced by magmatic injection

Carola Leva*, Georg Rümpker, Frederik Link, Ingo Wölbern

Institute of Geosciences, Goethe-University Frankfurt, Altenhöferallee 1, 60438 Frankfurt am Main, Germany

ARTICLE INFO

Article history:
Received 13 June 2019
Received in revised form 6 September 2019
Accepted 6 September 2019
Available online 7 September 2019

Keywords:
Fogo volcano
Mantle earthquakes
Magma migration
Fogo, Cape Verde
Volcano-tectonic earthquakes
Array seismology

ABSTRACT

Fogo volcano belongs to the Cape Verde hotspot and its most recent eruption occurred from November 2014 to February 2015. From January to December 2016 we operated a temporary seismic network and array on Fogo and were able to locate 289 earthquakes in total. Array analysis shows that most of the events occur within the crust at distances >25 km near the neighboring island of Brava. However, on 15th August 2016 the network recorded an isolated cluster of >20 earthquakes, 13 of which could be located beneath the southern part of Fogo. The differences between S- and P-wave arrival times at steep incidence clearly indicate focal depths between approximately 38 and 44 km whereas receiver-function analyses place the Moho discontinuity at depths between 11 and 14 km. Thus, the earthquakes are located well within the upper mantle directly beneath Fogo. In view of the elevated upper-mantle temperatures within a hotspot regime, we propose that fracturing induced by magmatic injection is the most likely cause for the observed deep earthquakes.

1. Introduction

The Cape Verde archipelago is located roughly 700 km west of the coast of Senegal in the Atlantic Ocean (see Fig. 1). The volcanism in this region originates from a mantle plume underlying an almost stationary tectonic plate (Courtney and White, 1986; Gripp and Gordon, 2002). Fogo, located in the SW of the archipelago, belongs to the younger islands (<6 Ma, Holm et al., 2008) and is the only volcano of Cape Verde with reported historical eruptions (Faria and Fonseca, 2014). Its eruptions are dominated by effusive and strombolian activity. The last one took place from November 2014 to February 2015 (González et al., 2015) and the time interval between eruptions is about 20 years (Faria and Fonseca, 2014).

Whereas Fogo is seismically rather quiet, high seismic activity has been reported around and beneath the neighboring island Brava (at a distance of about 20 km west of Fogo) and the Cadamosto seamount 20 km to the southwest of Brava (Grevemeyer et al., 2010; Vales et al., 2014). Little is known about the internal structure of Fogo volcano. In previous studies a possible link of the magma supply systems of Fogo and Brava has been discussed in relation to seismicity that occurs in between the islands (see e.g., Heleno and Fonseca (1999) and Hildner et al. (2011) for details). Specifically, it has been argued that the seismicity prior to the 1995 eruption of Fogo relates to magma transport from Brava towards Fogo. The orientation of eruptive fissures during this eruption supports this assumption. However, chemical analysis of phenocryst rims reveals a short-term storage in shallow reservoirs of magma within the crust below Fogo a few hours before eruption (Hildner et al., 2011; Hildner et al., 2012). The results indicate that historic and prehistoric eruptions were fed by magma ascending from different small reservoirs within the mantle at depths ranging from 15 to 30 km (Hildner et al., 2012). This is supported by petrological and geochemical data of the most recent eruption 2014–2015, indicating magma storage within the mantle at a depth of about 25.6 ± 5.5 km (Mata et al., 2017). Furthermore, the island of Fogo has not experienced any significant island-wide deformation before and during this eruption, which also points to a deeper source, likely >15 km (González et al., 2015).

To better constrain the source region of the magma supply system beneath Fogo and its relation to seismic activity we operated a seismic array at a distance of about 8 km from the southern rim of the Chã das Caldeiras from January to December 2016. To improve event detection and localization capabilities of the array, three additional broadband stations were deployed across the island (Fig. 1) in January 2016.

2. Data analysis and methods

Our network consists of ten seismic stations, three of which are equipped with broadband Trillium Compact seismometers and seven with short-period (4.5 Hz) geophones.

* Corresponding author.
E-mail address: leva@geophysik.uni-frankfurt.de (C. Leva).

https://doi.org/10.1016/j.jvolgeores.2019.106672

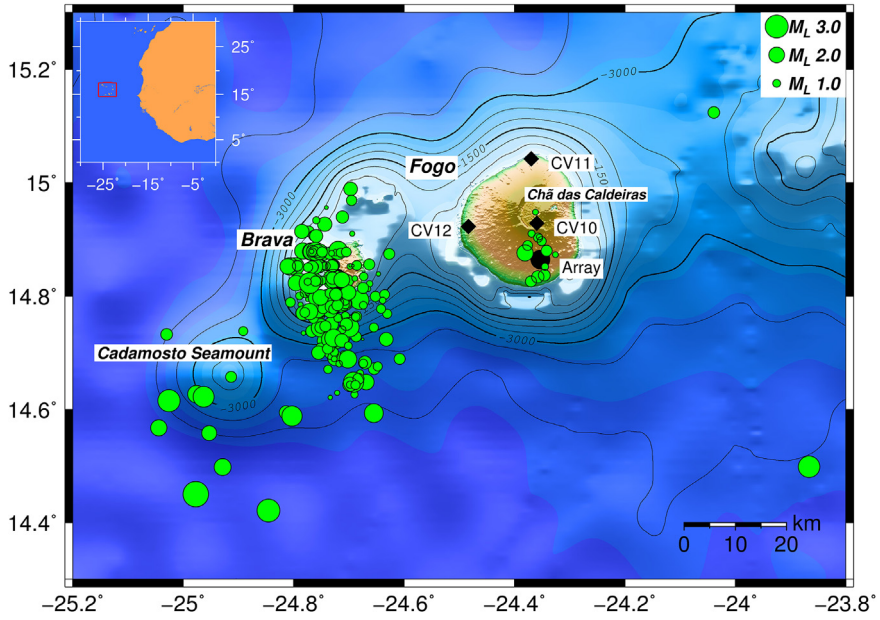

Fig. 1. Local seismicity between January 2016 and December 2016. Localized events exhibit magnitudes (M_L) between 0.3 and 3.0. The stations of the network are marked in black. Circle: Location of the array, which consists of 7 stations; Diamonds: additional broadband stations. Inset: Map of Cape Verde (marked in a red rectangle) and western African coastline. Topographic data including bathymetry are derived from the Global Multi-Resolution Topography Synthesis (Ryan et al., 2009). (For interpretation of the references to colour in this figure legend, the reader is referred to the web version of this article.)

The seven short-period instruments configure a seismic array with an aperture of 700 m, designed for the detection of local events with a mean frequency of about 7–10 Hz. The additional three broadband stations are distributed across the island, in the southern part of Chã das Caldeiras and in the northern and western parts of Fogo (e.g. Fig. 1). All stations were equipped with Omnirecs CUBE-dataloggers recording continuously with a sampling rate of 200 Hz. Data were collected from January to December 2016 with gaps of about 11 weeks in total due to storage limitations of the dataloggers. The longest gap of 4 weeks occurred in June and July.

Earthquakes that occurred outside of our network on Fogo are generally located using a time-domain array analysis. By performing a time-domain array analysis, information from a wide frequency band, implicitly, is incorporated, as the complete waveform is used in forming the beam. Traces are shifted and stacked to determine the beam energy for horizontal slownesses (s_x,s_y) in the range of ±3 s/km. From the horizontal slowness components at maximum energy the backazimuth of the event is derived and the absolute slowness yields the apparent velocity of the wavefront. Uncertainties of backazimuth and slowness are estimated by considering resulting variations in slowness obtained from a 5% reduction of the maximum energy. Epicentral distances are calculated from arrival-time differences between S- and P-waves. For local events at greater horizontal distance from the array (close to Brava or the Cadamosto seamount, Fig. 1), we assume a simplified two-layer model for the crust and underlying mantle with appropriate P-wave velocities taken from Vales et al. (2014), particularly 6.1 km/s for the crust and 8.0 km/s for the mantle. A fixed v_P/v_S-ratio of 1.74 is used. The Moho depth is set to 14 km in agreement with previous studies (e.g. Vales et al., 2014), while the events are assumed to occur at a fixed depth of 5 km, which is the mean depth of hypocenters beneath Brava (e.g., Faria and Fonseca, 2014). Some authors (Vales et al., 2014) have reported deeper events of about 10 km depth. Although we cannot directly constrain the earthquake depth from the array analysis, we obtain information about the maximum depth of the ray path from the horizontal slowness (ray parameter) derived from the analysis. In a laterally homogeneous medium, the ray parameter is constant, and its inverse (as determined from the apparent velocity across the array) corresponds to the velocity at the turning point of the ray. Thus, for distant earthquakes, the apparent velocity allows to discriminate between ray turning points within the crust and the mantle. For earthquakes observed around Brava, the apparent velocity of about 6 km/s is consistent with a crustal turning point (depth < 14 km). The error that may result from the deviation between the true earthquake depth relative to the fixed depth of 5 km has been carefully investigated and is covered by the error that we assume in the analysis (see below). From the theoretical arrival times for P and S waves (in the model), we derive differential arrival times as a function of distance which we compare with the measured time difference. This procedure is applied to all stations of the array, such that a mean distance is obtained. We apply an error of 10% to this distance to account for the uncertainties related to the depth and velocities used in the model.

For locating the earthquakes directly beneath Fogo we apply a standard localization method, HYPOCENTER (Lienert et al., 1986) (without any a priori depth constraints). We use the velocity model of Vinnik et al. (2012) derived for Santiago and Fogo. This model has the advantage that it provides a S-wave velocity structure derived from receiver functions. Details on the velocity model and its effects on the earthquake locations are given in the discussion below.

3. Results

Most of the events detected by our network exhibit the characteristics of volcano-tectonic (VT) earthquakes with clear P- and S-phases (see e.g. Wassermann (2012)) and occur beneath and around the island of Brava. There is also evidence for some long period volcanic events (naming in accordance to Fonseca et al., 2003) and more rarely harmonic “cigar-shaped” tremors with a length of several minutes to hours, but these events have not yet been localized. Fig. 1 shows the location of 289 earthquakes with magnitudes (M_L) 0.3 to 3.3, recorded between January and December 2016 that were located using either classical network or seismic array analysis (depending on the epicentral distance). Assuming an error of 5% of the maximum stacked energy in the

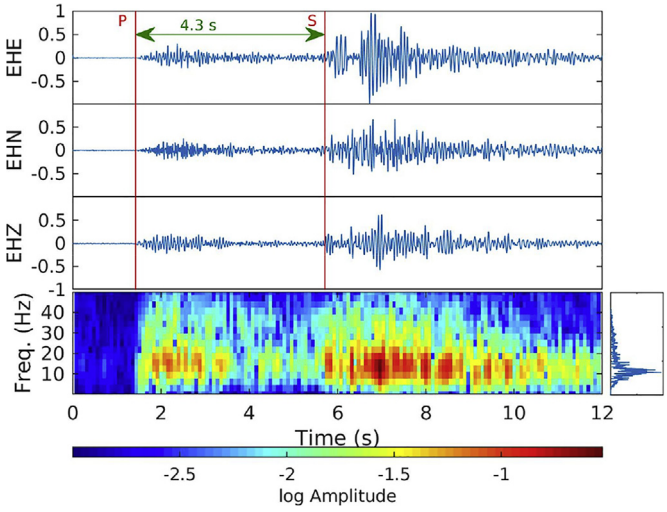

Fig. 2. Top: Three-component velocity seismograms of the event recorded on 15 August 2016 at 09:59 at a short-period station of the seismic array on Fogo. A Butterworth filter with cutoff frequencies of 0.1 and 50 Hz has been applied. Bottom left: Spectrogram of the record, bottom right: frequency content of the signal. Dominant frequencies are in the range from 10 Hz to 20 Hz.

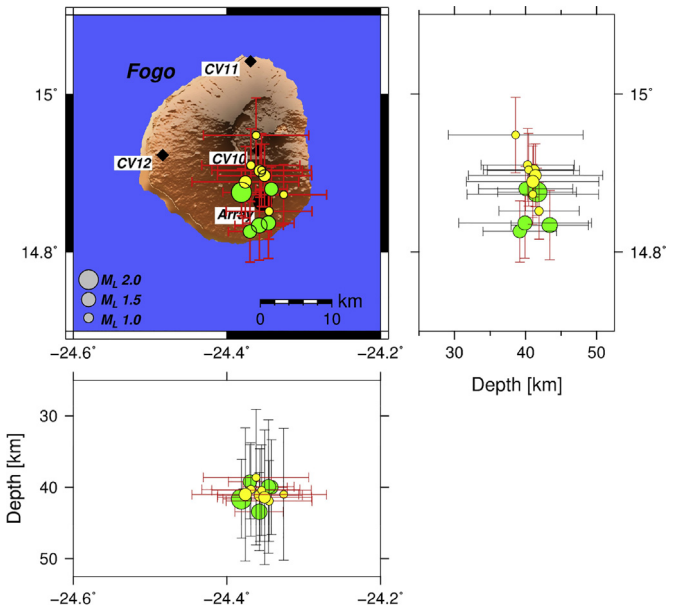

Fig. 3. Location of the swarm of deep events beneath Fogo on 15 August 2016. Magnitudes (M_L) range from 0.8 to 2.1. Yellow symbols: Localization performed without station CV11 due to poor data quality. Green symbols: Localization of earthquakes including the traces of CV11. Black circle: Location of the array, which consists of 7 stations; Black diamonds mark the positions of additional broadband stations. Horizontal error bars (in red) are derived from the localization using SEISAN, vertical error bars (in black) also account for uncertainties in the velocity (see main text). (For interpretation of the references to colour in this figure legend, the reader is referred to the web version of this article.)

array analysis leads to average errors of about ±10° for the backazimuth and ± 5–8 km for the distance estimations.

Detectable earthquakes beneath Fogo were recorded on 15 August. >20 of these occurred within 1 h, followed by some larger earthquakes during the next 10 h. Around the time of this earthquake swarm we do not observe any long period seismicity or tremors. We were able to locate 13 earthquakes of this swarm for which the seismograms exhibited a sufficiently high signal to noise ratio. A table of the analyzed events is given in the supplements. As an example, we show 3-component recordings for one of the stronger earthquakes (M_L 2.1) in Fig. 2. The events are generally characterized by dominant frequencies between 10 and 20 Hz. As the earthquakes occurred at depth directly beneath the stations, their focal mechanism could not be determined. Fig. 3 clearly indicates the clustering of the source locations, both, horizontally and vertically. The errors in latitude and longitude are of the order of ±4 to 5 km and ± 5 to 6 km, respectively. The depth of the events ranges from 38.6 km to 43.4 km, with a mean depth of 40.8 km. This is in agreement with the observed time differences between P- and S-wave arrivals of about 4.3 s. The error of the depth estimation is discussed below. There is no systematic change in depth and lateral position of the earthquakes over time.

The earthquakes do not follow a typical mainshock-aftershock sequence. Magnitudes (M_L) of the analyzed events range from 0.8 to 2.1. The events within the first hour reach a maximum magnitude of 1.2 whereas the events during the following 10 h reach magnitudes of up to 2.1. Support for the location of the earthquakes at depth directly beneath Fogo comes from seismograms recorded at the array stations. The traces show a negligible time shift and the maximum of the stacked energy corresponds to an apparent velocity that approaches infinity, consistent with a near-horizontal wavefront arriving at the array (Fig. 4). In comparison, the typical apparent velocity for an event originating around Brava is around 6.4 km/s. Further support for the steep incidence comes from the polarization analysis of the first P-wave arrivals as shown in Fig. S2.

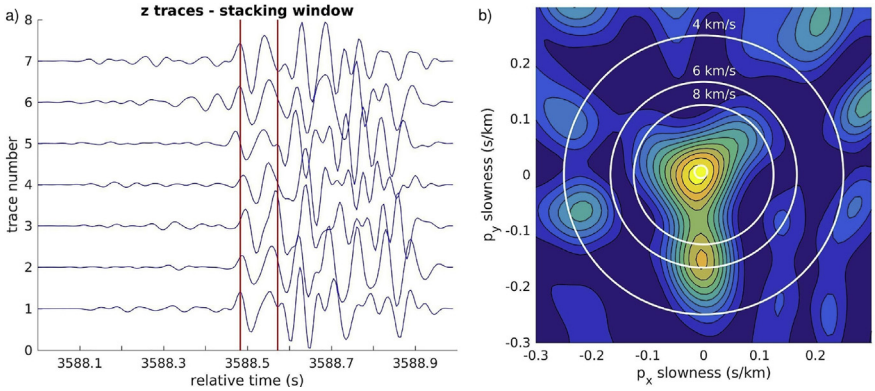

Fig. 4. Example of the array analysis applied to a deep event (at 09:59 on 15 August 2016) beneath Fogo. a) Traces before shifting and stacking. Traces of the seven array stations are filtered between 10 and 25 Hz. The larger time window has a length of 1 s, the smaller stacking window is marked in red. b) time-domain energy stack of the shifted traces. The resulting slowness value at the maximum corresponds to an apparent velocity approaching infinity. (For interpretation of the references to colour in this figure legend, the reader is referred to the web version of this article.)

4. Discussion

VT events beneath Fogo are relatively rare (Fonseca et al., 2003) and have been reported to occur at shallow depths <10 km (Heleno and Fonseca, 1999; Faria and Fonseca, 2014; Vales et al., 2014). The deep events beneath Fogo reported here are located south of Chã das Caldeiras and occur at a depth of about 40 km, whereas previous studies indicate crustal thickness of only about 12 to 14 km (Pim et al., 2008; Vinnik et al., 2012). We therefore conclude that the earthquakes are located well within the uppermost mantle. The error in our depth estimate obtained from the localization procedure is in the range of ±1.2 to 2.7 km. However, systematic errors that may arise from the choice of the velocity model are not accounted for in this estimate. Therefore, to allow for a wider range of realistic velocities, we also consider velocity profiles that have been derived for some of the Canary Islands (Lodge et al., 2012). The velocity structure found there may provide additional information for the possible velocity variations in a hot spot regime. A standard deviation for the earthquake depth is then estimated from the different results obtained for all velocity models considered (for the Canary Islands and Cape Verde), including those used earlier (Vinnik et al. (2012) and Vales et al. (2014)). The resulting uncertainties of the compilation of velocity models range from ±5.2 to 9.5 km in depth, depending on the event, and are given in Fig. 3. Additional application of a double-difference earthquake location method (hypoDD, Waldhauser (2001)) does not significantly change earthquake locations and confirms the previous depth estimates. Due to its relatively high noise level, data of station CV11 had to be discarded from the analysis of some events. In Fig. 3 the colour code indicates whether CV11 was included to determine a specific event location. To test the influence of station CV11, the localization procedure for all events was repeated by excluding data from this station. In this case, locations of the earthquakes are shifted systematically by about 1 km towards the North-East, while the effect on the depth estimates is negligible. However, the horizontal shift is well within the error range derived earlier.

To further confirm the subcrustal origin of the earthquakes we also performed a separate receiver function analysis for Fogo, for which we used the data collected at two of the broadband stations, CV10 and CV12, whereas CV11 was not used due to its higher noise level. In addition, we included the data of five temporary stations of the COBO network which was operating on Fogo during 2007 and 2008 (see Vinnik et al., 2012). We used the method of Zhu and Kanamori (2000) to constrain the crustal thickness H and the bulk v_P/v_S ratio of the crust beneath Fogo. For more information about data quality and preparation we refer to the supplementary material. The analysis leads to values of 11.1 ± 4.5 km for the crustal thickness and to 1.73 ± 0.12 for the velocity ratio (see Fig. S6) which is in agreement with the previous results (Pim et al., 2008; Vinnik et al., 2012) mentioned above.

Previously, Vales et al. (2014) reported different occurrences of deeper earthquakes in the region, some of them at depths close to 40 km. Several events occurred about 30 km offshore close to a field of volcanic cones southwest of Santo Antão, the northernmost island of Cape Verde (approximately 220 km north of Fogo), others in the vicinity of the Cadamosto seamount, southwest of Brava. Additionally, some isolated earthquakes at depths between 20 and 30 km occurred offshore, west of Brava. However, the corresponding depth estimates are not well constrained because of the offshore locations of these events resulting in a large azimuthal gap; a relation to the magmatic activity beneath Fogo cannot be established.

The temperature in the upper mantle beneath Cape Verde is likely too high to support fracturing, unless induced by magmatic injection to produce the required high strain rates. The crust of Cape Verde is about 125–150 Ma old (Pim et al., 2008). The corresponding temperature within the oceanic lithosphere (without a mantle plume) at this age and at a depth of 40 km falls within the range of 450°-500 °C (McKenzie et al., 2005). Wilson et al. (2013) compare the excess temperature of Cape Verde with the excess temperature of Hawaii, which is about 300 °C. Thus, we can assume a temperature of approximately 750 °C at the depth of the earthquakes beneath Fogo. This is significantly higher than the temperature of 650 °C for the transition from brittle to ductile behavior (as defined in Schmeling and Marquart, 2008). Even when considering a more moderate value for the excess temperature of 200 °–250 °C (see White, 2010) the earthquakes must be induced by magmatic processes.

As a likely explanation for the subcrustal events beneath Fogo we therefore suggest the rapid movement of magma into the shallower upper mantle, possibly into a reservoir where it accumulates before the next eruption. Similar processes have been observed for example in Hawaii (Wright and Klein, 2006) and at Piton de la Fournaise (Michon et al., 2015). At Bárðarbunga (Iceland) Hudson et al. (2017) report earthquakes in the ductile part of the crust, which they attributed to melt-induced brittle failure. Considering the location of the events directly beneath Fogo, the hypothesis of a common magma supply system for Fogo and Brava, as discussed in previous studies (see e.g., Heleno and Fonseca (1999), Fonseca et al. (2003), for details), now seems less likely. Observations of earthquakes in the region between Brava and Fogo, as well as the orientation of eruptive fissures led to this assumption. Two separated supply systems with an independent magma storage beneath Fogo, as also suggested by petrological studies (Hildner et al., 2011), may explain the isolated deep events better. Based on thermobarometric analyses, Hildner et al. (2012) propose magma reservoirs related to historic and prehistoric eruptions at depths between 15 and 30 km.

In view of these estimates, the newly observed events may indicate magma transport from a deeper source into an accumulation zone at depths of about 40 km. Although these processes occur below the brittle crust, rapid movement of magma can lead to strain rates high enough to cause magmatic fracturing and seismicity in normally aseismic zones. Possible processes can be the breaking up and pushing of plugs along a dyke or faulting at the tip of the dyke (White et al., 2011). Tarasewicz et al. (2012) suggest that overpressure in a sill causes magma to escape under high strain rates through a bottleneck, where seismicity originates. Generally, the deep events beneath Fogo exhibit very similar waveforms. However, a systematic analysis of first-motion polarities remains inconclusive due to the relatively low signal-to noise ratio of the first arrivals. The observed distances between the individual deep earthquakes are likely overestimated due to uncertainties resulting from the localization procedure and hence the fracturing may be limited to a smaller domain. The scarcity of the deep events beneath Fogo may suggest that the molten material generally moves under aseismic conditions. Tarasewicz et al. (2012) argue that changes in flow conditions can result in clogged up pathways, leading to a transition from aseismic to seismic movement of magma.

A downward migration of relaxation through the plumbing system can also explain the occurrence of these events after the eruption (Michon et al., 2015). The absence of earthquakes beneath Fogo in the depth range between about 10 and 40 km may be related to aseismic movement of magma or an aseismic zone caused by melt accumulation. At Piton de la Fournaise, Michon et al. (2015) observe a seismic gap between 8 and 11 km and address this to a zone of magma storage. White et al. (2011) discuss a possible freezing of magma at depth and the aseismic storage in sills in the northern volcanic rift zone in Iceland. Tarasewicz et al. (2012) observe several earthquake clusters beneath Eyjafjallajökull in Iceland at different depths with gaps of a few kilometers between

them and assign a fracturing process of solidified magma in an aseismic melt conduit. The cooling magma model of Aso and Tsai (2014) explains the occurrence of deep seismic events characterized by relatively low frequencies (DLP events). In view of the high frequency content of the earthquakes beneath Fogo, we consider magmatic injection processes to be more significant for our observations.

5. Conclusions

From January to December 2016 we operated a seismic network and array on Fogo, Cape Verde. Most of the seismicity recorded originates from sources at crustal depths beneath or around Brava. We detected a group of earthquakes directly beneath Fogo at depths ranging between 38.6 and 43.4 km, clustering locally and in time. The majority of the earthquakes occurred within one hour with mean magnitudes of 0.9, followed by slightly stronger events during the next 10 h, without a systematic shift in depth over time. In comparison to e.g. the seismic activity near Brava, previous studies show very few earthquakes below Fogo, which were located within the crust down to depths of about 10 km.

The seismic gap observed at Fogo ranges from about 10 km down to 40 km which is probably best explained by a large-scale magma accumulation zone. Post-eruptive seismicity has been observed at several other ocean volcanoes. For example, at El Hierro several clusters of seismicity in the lower crust and upper mantle showed a migration that was explained by magmatic intrusions, in conjunction with a significant uplift of the island (Klügel et al., 2015; Benito-Saz et al., 2017).

We conclude that the earthquakes likely originate from magma injection into a deep subcrustal reservoir. Two possible mechanisms, that are capable to generate high strain rates and can explain the temporal and spatial clustering of the earthquakes, are the fracture of a solidified magma plug within a dyke or the opening of a new dyke, where earthquakes occur at its tip (White et al., 2011). Because of the high strain rates generated by these processes, fracturing can occur even within normally ductile zones of the upper mantle. In view of the new results and of petrological studies (Hildner et al., 2011), a previously-proposed common source for the shallow magma plumbing system of Fogo and its neighboring island Brava seems less likely and requires further investigation.

Declaration of competing interest

None.

Acknowledgments

This study has been supported by funds from Goethe University Frankfurt am Main and by a grant from Deutsche Forschungsgemeinschaft (DFG) to Ingo Wölbern (grant number WO 1723/3-1). Some of the seismic stations for this study were provided by the Geophysical Instrument Pool Potsdam. We are very grateful to Bruno Faria for his support in making this project possible. We thank José Levy for logistic support and customs handling. Paulo Fernandes Teixeira and José Antonio Fernandes Dias Fonseca are thanked for the support during field work. We further thank the reviewers for their comments and suggestions which helped to improve the manuscript.

Appendix A. Supplementary data

Supplementary data to this article can be found online at https://doi.org/10.1016/j.jvolgeores.2019.106672.

References

Aso, N., Tsai, V., 2014. Cooling magma model for deep volcanic long-period earthquakes. J. Geophys. Res. Solid Earth 119, 8442–8456, http://dx.doi.org/10.1002/2014JB011180.

Benito-Saz, M.A., Parks, M.M., Sigmundsson, F., Hooper, A., García-Cañada, L., 2017. Repeated magmatic intrusions at El Hierro Island following the 2011–2012 submarine eruption. J. Volcanol. Geotherm. Res. 344, 79–91, http://dx.doi.org/10.1016/j.jvolgeores.2017.01.020.

Courtney, R.C., White, R.S., 1986. Anomalous heat flow and geoid across the Cape Verde Rise: evidence for dynamic support from a thermal plume in the mantle. Geophys. J. R. Astron. Soc. 87, 815–867, http://dx.doi.org/10.1111/j.1365-246X.1986.tb01973.x.

Faria, B., Fonseca, J.F.B.D., 2014. Investigating volcanic hazard in Cape Verde Islands through geophysical monitoring: network description and first results. Nat. Hazards Earth Syst. Sci. 14, 485–499, http://dx.doi.org/10.5194/nhess-14-485-2014.

Fonseca, J.F.B.D., Faria, B.V.E., Lima, N.P., Heleno, S.I.N., Lazaro, C., d'Oreye, N.F., Ferreira, A.M.G., Barros, I.J.M., Santos, P., Bandomo, Z., Day, S.J., Osorio, J.P., Baio, M., Matos, J.L.G., 2003. Multiparameter monitoring of Fogo Island, Cape Verde, for volcanic risk mitigation. J. Volcanol. Geotherm. Res. 125, 39–56, http://dx.doi.org/10.1016/S0377-0273(03)00088-X.

González, P.J., Bagnardi, M., Hooper, A.J., Larsen, Y., Marinkovic, P., Samsonov, S.V., Wright, T.J., 2015. The 2014-2015 eruption of Fogo volcano: Geodetic modeling of Sentinel-1 TOPS interferometry. Geophys. Res. Lett. 42, 9239–9246, http://dx.doi.org/10.1002/2015GL066003, v.

Grevemeyer, I., Helffrich, G., Faria, B., Booth-Rea, G., Schnabel, M., Weinrebe, W., 2010. Seismic activity at Cadamosto seamount near Fogo Island, Cape Verdes – formation of a new ocean island? Geophys. J. Int. 180, 552–558, http://dx.doi.org/10.1111/j.1365-246X.2009.04440.x.

Gripp, A.E., Gordon, R.G., 2002. Young tracks of hotspots and current plate velocities. Geophys. J. Int. 150, 321–361, http://dx.doi.org/10.1046/j.1365-246X.2002.01627.x.

Heleno, S.I.N., Fonseca, J.F.B.D., 1999. A seismological investigation of the Fogo Volcano, Cape Verde Islands: preliminary results. J. Volcanol. Seismol. 20, 199–217.

Hildner, E., Klügel, A., Hauff, F., 2011. Magma storage and ascent during the 1995 eruption of Fogo, Cape Verde Archipelago. Contrib. Mineral. Petrol. 162, 751–772, http://dx.doi.org/10.1007/s00410-011-0623-6.

Hildner, E., Klügel, A., Hansteen, T.H., 2012. Barometry of lavas from 1951 eruption of Fogo, Cape Verde Islands: Implications for historic and prehistoric magma plumbing systems. J. Volcanol. Geotherm. Res. 217-218, 73–90, http://dx.doi.org/10.1016/j.jvolgeores.2011.12.014.

Holm, P.M., Grandvuinet, T., Friis, J., Wilson, J.R., Barker, A.K., Plesner, S., 2008. An ^{40}Ar-^{39}Ar study of the Cape Verde hot spot: Temporal evolution in a semistationary plate environment. J. Geophys. Res. 113, B08201, http://dx.doi.org/10.1029/2007JB005339.

Hudson, T.S., White, R.S., Greenfield, T., Ágústsdóttir, T., Brisbourne, A., Green, R.G., 2017. Deep crustal melt plumbing of Bárðarbunga volcano, Iceland. Geophys. Res. Lett. 44, 8785–8794, http://dx.doi.org/10.1002/2017GL074749.

Klügel, A., Longpré, M.-A., García-Cañada, L., Stix, J., 2015. Deep intrusions, lateral magma transport and related uplift at ocean island volcanoes. Earth Planet. Sci. Lett. 431, 140–149, http://dx.doi.org/10.1016/j.epsl.2015.09.031.

Lienert, B.R., Berg, E., Frazer, L.N., 1986. HYPOCENTER: An earthquake location method using centered, scaled, and adaptively damped least squares. Bull. Seismol. Soc. Am. 76, 771–783.

Lodge, A., Nippress, S.E.J., Rietbrock, A., Gracía-Yeguas, A., Ibáñez, J.M., 2012. Evidence for magmatic underplating and partial melt beneath the Canary Islands derived using teleseismic receiver functions. Phys. Earth Planet. Inter. 212, 44–54, http://dx.doi.org/10.1016/j.pepi.2012.09.004, v.

Mata, J., Martins, S., Mattielli, N., Madeira, J., Faria, B., Ramalho, R.S., Silva, P., Moreira, M., Caldeira, R., Moreira, M., Rodrigues, J., Martins, L., 2017. The 2014–15 eruption and the short-term geochemical evolution of the Fogo volcano (Cape Verde): Evidence for small-scale mantle heterogeneity. Lithos 288-289, 91–107, http://dx.doi.org/10.1016/j.lithos.2017.07.001.

McKenzie, D., Jackson, J., Priestley, K., 2005. Thermal structure of oceanic and continental lithosphere. Earth Planet. Sci. Lett. 233, 337–349, http://dx.doi.org/10.1016/j.epsl.2005.02.005.

Michon, L., Ferrazzini, V., Di Muro, A., Villeneuve, N., Famin, V., 2015. Rift zones and magma plumbing system of Piton de la Fournaise volcano: How do they differ from Hawaii and Etna? J. Volcanol. Geotherm. Res. 303, 112–129, http://dx.doi.org/10.1016/j.jvolgeores.2015.07.031.

Pim, J., Peirce, C., Watts, A.B., Grevemeyer, I., Krabbenhoeft, A., 2008. Crustal structure and origin of the Cape Verde Rise. Earth Planet. Sci. Lett. 272, 422–428, http://dx.doi.org/10.1016/j.epsl.2008.05.012.

Ryan, W.B.F., Carbotte, S.M., Coplan, J.O., O'Hara, S., Melkonian, A., Arko, R., Weissel, R.A., Ferrini, V., Goodwillie, A., Nitsche, F., Bonczkowski, J., Zemsky, R., 2009. Global Multi-Resolution Topography synthesis. Geochem. Geophys. Geosyst. 10, Q03014, http://dx.doi.org/10.1029/2008GC002332.

Schmeling, H., Marquart, G., 2008. Crustal accretion and dynamic feedback on mantle melting of a ridge centred plume: The Iceland case. Tectonophysics 447, 31–52, http://dx.doi.org/10.1016/j.tecto.2006.08.012.

Tarasewicz, J., Bransdóttir, B., White, R.S., Hensch, M., Thorbjarnardóttir, B., 2012. J. Geophys. Res. 117, B00C06, http://dx.doi.org/10.1029/2011JB008751, Using microearthquakes to track repeated magma intrusions beneath the Eyjafjallajökull stratovolcano, Iceland.

Vales, D., Dias, N.A., Rio, I., Matias, L., Silveira, G., Madeira, J., Weber, M., Carrilho, F., Haberland, C., 2014. Intraplate seismicity across the Cape Verde swell: A contri-

bution from a temporary seismic network. Tectonophysics 636, 325–337, http://dx.doi.org/10.1016/j.tecto.2014.09.014.
Vinnik, L., Silveira, G., Kiselev, S., Farra, V., Weber, M., Stutzmann, E., 2012. Cape Verde hotspot from the upper crust to the top of the lower mantle. Earth Planet. Sci. Lett. 319-320, 259–268, http://dx.doi.org/10.1016/j.epsl.2011.12.017.
Waldhauser, F., 2001. HypoDD: A computer program to compute double-difference earthquake locations. USGS Open File Rep., 01–113.
Wassermann, J., 2012. Volcano Seismology. In: Bormann, P. (Ed.), New Manual of Seismological Observatory Practice 2 (NMSOP-2), Potsdam: Deutsches GeoForschungsZentrum GFZ. , pp. 1–77, http://dx.doi.org/10.2312/GFZ.NMSOP-2_ch13.
White, R.S., Drew, J., Martens, H.R., Key, J., Soosalu, H., Jakobsdóttir, S.S., 2011. Dynamics of dyke intrusion in the mid-crust of Iceland. Earth Planet. Sci. Lett. 304, 300–312, http://dx.doi.org/10.1016/j.epsl.2011.02.038.
White, W.M., 2010. Oceanic Island Basalts and Mantle Plumes: The Geochemical Perspective. Annu. Rev. Earth Planet. Sci. 38, 133–160, http://dx.doi.org/10.1146/annurev-earth-040809-152450.
Wilson, D.J., Peirce, C., Watts, A.B., Grevemeyer, I., 2013. Uplift at lithospheric swells—II: is the Cape Verde mid-plate swell supported by a lithosphere of varying mechanical strength? Geophys. J. Int. 193, 798–819, http://dx.doi.org/10.1093/gji/ggt034.
Wright, T.L., Klein, F.W., 2006. Deep magma transport at Kilauea volcano, Hawaii. Lithos 87, 50–79, http://dx.doi.org/10.1016/j.lithos.2005.05.004.
Zhu, L., Kanamori, H., 2000. Moho depth variation in southern California from teleseismic receiver functions. J. Geophys. Res. 105, 2969–2980, http://dx.doi.org/10.1029/1999JB900322.